22nd Australasian Fluid Mechanics Conference AFMC2020
Brisbane, Australia, 6-10 December 2020
DOI: 10.14264/uql.2020.xxyy

Modelling pheromone flow from insect traps

S. Chen[1], R. Horner[2], D M Suckling[2], T Strand[3] and M Jermy[1]

[1]Department of Mechanical Engineering, University of Canterbury, Christchurch 8140, New Zealand

[2]The New Zealand Institute for Plant and Food Research Limited, Christchurch 8140, New Zealand

[3]New Zealand Forest Research Institute Limited, Christchurch 8140, New Zealand

Abstract

The Brown Marmorated Stink Bug (BMSB) *Halyomorpha halys* is an unwanted invasive species. Its entry and establishment in New Zealand would result in significant production impacts in the horticultural industry. Current BMSB traps are A4 size sticky panels with aggregation pheromone as a lure. These traps are affordable, but inefficient. A novel live trap has been proven ~7 times as efficient in a forest–vineyard margin in Italy. This trap has the lure in the trap chamber and self-orients to the wind. The present work used CFD to model pheromone transport, comparing the sticky panel to the new trap, and to a refined design suitable for mass production. The new trap produces a more concentrated plume than the panel traps. Pheromone dispersion is compared in three environments (flat plain, car yard and vegetation). The pheromone plume mixes more rapidly in vegetation. The current results use a coarse mesh, but guide further modelling and design refinement.

Keywords

Insect pheromone; vapour transport; atmospheric boundary layer; biosecurity

Introduction

The Brown Marmorated Stink Bug (BMSB) *Halyomorpha halys* is native to China, Japan, Korea and Taiwan, and has spread to several countries in North America and Europe where it has become a major agricultural pest for several crops. It has not yet been reported in New Zealand, but is regularly intercepted at the border, and would cause severe economic loss if established. Routine surveillance at high-risk locations uses A4 sticky panels above which a high dose lure (Trécé, Adair, OK, USA) is suspended (Figure 1).

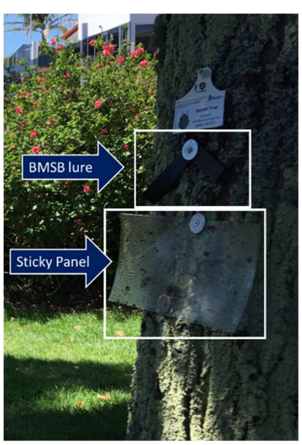

Figure 1. Sticky panel trap with lure (the black strip) above it.

The lure contains the BMSB aggregation pheromone plus the *Plautia stali* brown-winged green stink bug aggregation pheromone as a synergist. The system of lure and panel alone is inefficient, and beating of the vegetation surrounding the trap is required. Suckling et al. [1] designed a novel live trap which addresses some shortcomings of the sticky panels. The trap consists of a duct, suspended in the wind, and oriented by means of a tail vane (Figure 2).

Figure 2. The original live trap developed by Suckling et al. [1].

A pheromone lure (identical to those used with the sticky panels) is suspended inside the duct. The upstream end of the duct is fitted with a mesh which prevents bugs from escaping. The downstream end also has a mesh, formed into a cone with an open tip. Nearby bugs follow the plume of pheromone carried on the wind from the trap, enter the downstream cone, and climb up it towards the pheromone source. Once inside, they lack the motivation and the spatial awareness to find the entrance hole and leave the trap. Trials in forest-vineyard margins in Italy showed this type of trap to accumulate BMSB at ~7 times the rate of sticky panel traps [1]. Since then, the trap design has been refined for cost-effective manufacture. This paper describes modelling to gain a preliminary understanding of the dispersion of the pheromone plume.

Development of the trap design

An ideal trap yields a high concentration of pheromone in the flow exiting the trap, is inexpensive to manufacture, and is robust in wind, rain and sun. The original prototype proved highly effective but was time-consuming to assemble. A new prototype was developed (Fig. 3). The trap body is made of a single sheet of 1 mm thick black polypropylene. Tabs, slots and holes for easy assembly and hanging are cut into the sheet. The vane is cut from Corflute (twin-walled cellular polypropylene carton board). The meshes are cut from 5 mm spaced polypropylene mesh (Quadra 05, Tenax, Baltimore, MD, USA). Laser cutting was used for the small test batch, but die cutting would be cost effective at volume. Each trap can be assembled in a few minutes using cable ties and spring clips. Measurements in the wind tunnel at showed that the air speed at the trap exit was 70% of the wind speed at 0.5 m/s. At the time of writing, the revised traps are being tested in vineyard margins in Italy.

Figure 3. New prototype trap.

CFD methodology

The flow was modelled with the COMSOL Multiphysics® 5.5 [2] time-dependent, segregated solver. The geometry was initially meshed with default physics-controlled settings, and later, mesh refinement in all boundary layers. Typical meshes contain 35-60,000 nodes, which are not converged, but are sufficient for an initial exploration of the factors which dominate the flow.

Governing equations and boundary conditions for air flow

Air flow is modelled with the incompressible continuity (Eq. 1) and Navier-Stokes equations (Eq. 2):

$$\nabla \cdot \boldsymbol{u} = 0 \tag{1}$$

$$\rho\frac{\partial \boldsymbol{u}}{\partial t} + \rho(\boldsymbol{u}\cdot\nabla)\boldsymbol{u} = -\nabla p + \mu\nabla^2\boldsymbol{u} + \frac{1}{3}\mu\nabla(\nabla\cdot\boldsymbol{u}) + \boldsymbol{F} \tag{2}$$

where ρ is the density of air, $\boldsymbol{u}$ is the velocity vector, t is time, p is pressure, and the external force $\boldsymbol{F}$ is assumed to be negligible. The air is assumed isothermal. The boundary conditions for air transport are:

- Upstream boundary – Inlet with uniform flow of velocity $\boldsymbol{u_0} = (0.57\ \text{m/s}, 0, 0)$. The low speed is chosen as adult BMSB only fly in light winds.
- Top boundary and vertical boundary facing the viewer in Figs. 4-8 – Open boundary, i.e. $\left[-\nabla p + \mu\nabla^2\boldsymbol{u} + \frac{1}{3}\mu\nabla(\nabla\cdot\boldsymbol{u})\right]\boldsymbol{n} = -f_0\boldsymbol{n}$, where $\boldsymbol{n}$ is the normal vector and the normal stress $f_0 = 0$.
- Bottom boundary (ground) – No slip wall
- Symmetry on a vertical plane through the trap axis
- Downstream boundary – Outlet, i.e. $\left[-\nabla p + \mu\nabla^2\boldsymbol{u} + \frac{1}{3}\mu\nabla(\nabla\cdot\boldsymbol{u})\right]\boldsymbol{n} = -p_0\boldsymbol{n}$, where the pressure p_0 at the boundary is assumed to be zero.

The governing equations are solved using the Discontinuous Galerkin finite element method. The reference pressure and temperature are 1 atm and 300 K.

At wind speeds of 0.5 m/s or more, the flow inside and outside the trap is turbulent. For most of the results below, the RANS $\mathrm{k}-\varepsilon$ model was used with inlet turbulent intensity 50%, and turbulence length scale is 3.8% of the domain height or the diameter of the trap exit. Large eddy simulation (LES) was used for two simulations, with the Residual Based Variational Multiscale (RBVM) method.

Governing equations and boundary conditions for the transport modelling of pheromone

Pheromone transport is modelled with Eq. 3:

$$\frac{\partial c}{\partial t} + \boldsymbol{\nabla}\cdot\left(-D\nabla c + j_{\text{evap}}\right) + \overline{\boldsymbol{u}}\cdot\nabla c = 0 \tag{3}$$

where c is the concentration of the pheromone, D the diffusion coefficient, and $\overline{\boldsymbol{u}}$ the mass averaged velocity. j_{evap} is the flux of pheromone leaving the surface of the lure and entering the air flow.

The diffusion coefficient of the pheromone has not been measured. A value of 3.6×10^{-8} m^2/s was estimated by scaling the diffusion coefficient of air at 20°C by the cube root of molecular mass.

The release rate of the pheromone is not known. Each lure is estimated to contain less than 5 micro moles of pheromone, and to be potent for twelve weeks under normal conditions. Release rates are expected to be in the pico to femto mole per hour. Weighing is not sensitive enough to measure release rates, and gas chromatography required more sensitive equipment than was available. It was assumed that the flux leaving the lure surface (j_{evap}) could be modelled as an evaporation process with fixed release rate coefficient K_{evap} and saturation vapour pressure c_e (Eq. 4):

$$j_{\text{evap}} = K_{\text{evap}}(c_e - c) \tag{4}$$

Arbitrary values of $c_e = 1\frac{mol}{m^3}$ and $K_{\text{evap}} = 1000\frac{m}{s}$ were chosen. These are guesses, and further, the concentrations which BMSB is sensitive to is not yet known. Nevertheless, the resulting models allow comparisons between the pheromone plumes propagating from different traps.

The boundary conditions in the transport modelling of pheromone are summarised below:

- Upstream boundary – Fixed concentration $c = 0$.
- Lure surface – Source surface j_{evap}.
- Upper boundary – Open, i.e. $-\boldsymbol{n}\cdot(-D\nabla c) = 0$ if $\boldsymbol{u}\cdot\boldsymbol{n} \geq 0$ (outflow), or $c = 0$ if $\boldsymbol{u}\cdot\boldsymbol{n} < 0$ (inflow).
- Symmetry on a vertical plane through the trap axis.
- Vertical boundary facing the viewer in Figs. 4–8 – Open.
- Downstream boundary – Outlet, i.e. equivalent to the outflow case of the open boundary.
- Bottom and other remaining boundaries – Zero flux, i.e. $-\boldsymbol{n}\cdot(-D\nabla c + \boldsymbol{u}c) = 0$.

Results: pheromone dispersion from the sticky panel, original and redeveloped traps

It is assumed that, for the original and new trap, the exit air velocity is 0.28 m/s and 0.40 m/s respectively. These values are obtained by taking the average exit velocity predicted by a CFD model which did not include the plastic meshes, multiplied by a correction factor of 0.7 for the plastic meshes, which was measured in a wind tunnel.

The pheromone concentrations, on a log scale, are shown in Figs. 4-8. Figs. 4-6 show the sticky panel with a 100 x 20 mm lure mounted above the A4 sticky panel. The lure and panel are fixed to a cylinder representing a tree trunk. They are 1.49 m above the ground. The wind speed is 0.57 m/s. $\mathrm{k}-\varepsilon$ RANS was used. In Fig. 4 the lure and panel are on side of the tree (the wind blows parallel to the panel face). In Fig. 5 the lure and panel are on the upwind side, in Fig. 6 on the downwind side. The pheromone plume depends strongly on wind direction.

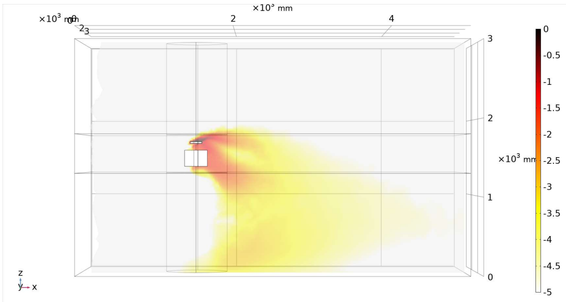

Figure 4. Plume concentration with the lure and A4 sticky panel on the side of the tree, with the wind blowing parallel to the panel face.

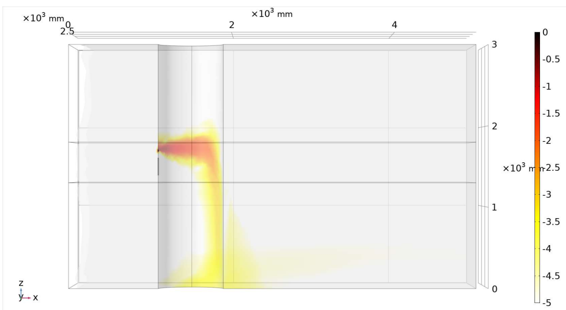

Figure 5. Plume concentration with the lure and panel on the upstream side of the tree.

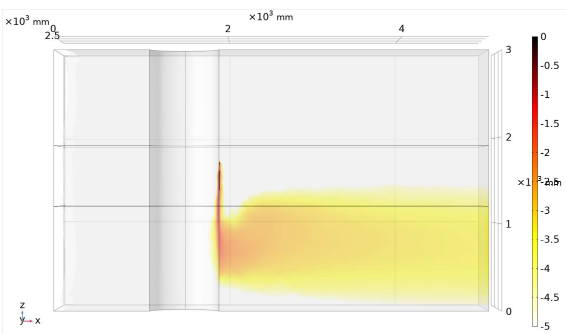

Figure 6. Plume concentration with the lure and panel on the downstream side of the tree.

Figs. 7 and 8 show the pheromone concentration for the original (Fig. 7) and new (Fig. 8) live trap. LES was used. In direct comparisons of LES and RANS models, the rate of lateral spread of the plume was similar. As these traps self-orient to the wind, the wind direction does not change the pheromone distribution. Compared to the sticky panel, the plume from the self-orienting traps is more concentrated, and is unidirectional. This means an insect following the gradient will always move towards the trap, except where there are gaps in the plume due to turbulent mixing. The new trap (Fig. 8) shows a slightly narrower and more concentrated plume than the original (Fig. 7). Air exiting the trap is slowed by wall friction, and interacts with the air flowing along outer surface to create a shear layer which broadens the pheromone plume. This effect is more pronounced with the divergent-convergent outer surface of the original trap than the straight sides of the new trap.

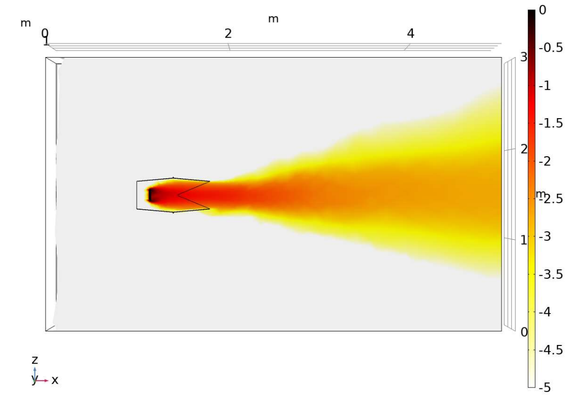

Figure 7 Plume concentration with the original trap.

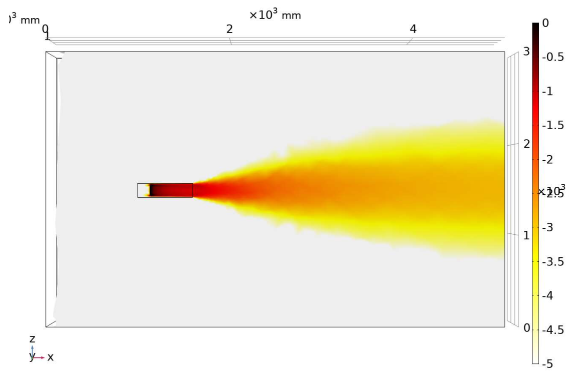

Figure 8. Plume concentration with the new trap.

Modelling of the dispersion of the pheromone plume from a simplified trap

In this section, the trap was simplified by placing the trap exit at the upstream boundary, and modelling it as a circular source region with an air velocity equal to 70% of the wind velocity. It is modelled in three different environments in which the trap is expected to be used. A flat and featureless plain is modelled by applying the default wall boundary condition on the bottom domain surface. A car storage yard is modelled by defining an array of blocks with 2 m in length, 1 m in height and 1 m in width, 0.4 m away from the ground (the car wheels are ignored), 0.5 m apart. A vegetation canopy is modelled by defining three arbitrarily located porous cylindrical "bushes" on the bottom domain surface. The wind profile of the atmospheric boundary layer u_{wind} was modelled with a power law (Eq. 5):

$$u_{\mathrm{wind}} = u_r \left(\frac{z}{z_r}\right)^{\alpha} \tag{5}$$

where z is the height, $u_r = 0.75\ \mathrm{m/s}$ is the reference wind speed at the reference height $z_r = 10\ m$, and $\alpha = 0.143$ is the empirical coefficient. Other boundary conditions are as described previously.

Modelling transport in the vegetation canopies

The canopies are modelled as porous media. It is assumed that the total mass of air inside the porous medium is conserved (i.e. the consumption or generation of gas by the vegetation is negligible within the timescale of interest), and the air properties in the continuum and porous medium domains are identical. Coupling Eq. 2 with Darcy's law yields Eq. 6 and 7:

$$\frac{\partial}{\partial t}(\phi\rho) + \nabla \cdot (\rho \boldsymbol{u}_p) = 0 \quad (6)$$

$$\boldsymbol{u}_p = -\frac{\kappa}{\mu}\nabla p_p \quad (7)$$

where $\boldsymbol{u}_p$ is the air velocity inside the porous medium, p_p is the pressure, $\phi = 0.5$ is the porosity, $\kappa = 0.01\ \mathrm{m}^2$ is the permeability, and. These values are initial guesses, and later, parameters will be taken from [3] in which a tomato plant canopy in a hothouse is modelled.

To couple the continuum and the porous medium domains, the inlets of the porous medium domains are defined as the outlets of the continuum domain, and vice versa, and setting $p = p_p$ at the boundaries of the porous medium.

Results: Terrain comparison

The predicted pheromone plume concentrations are shown in Figs. 9-11 below respectively, with concentration on a log scale. The trap is 0.8 m above the ground. At greater heights, the plume did not penetrate to the same degree into the canopies or the gaps between the cars.

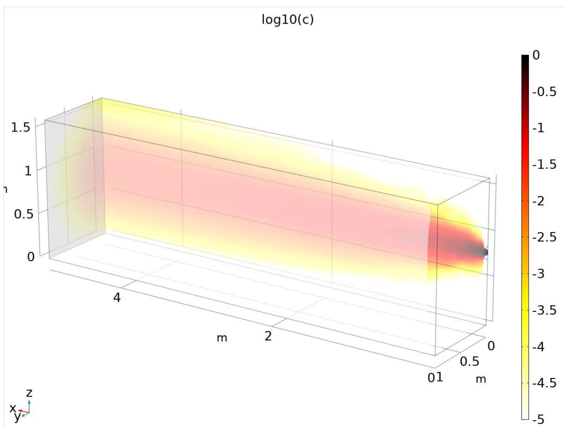

Figure 9. Plume concentration above the featureless plain.

Compared to the featureless plain, the car yard and vegetation canopies show, as expected, more complex pheromone distribution. The concentration gradient is broadly unidirectional, though there are exceptions. Mixing with air is enhanced in the gaps between the cars and within each vegetation canopy. The behaviour of BMSB when they encounter a local maximum in pheromone concentration or a gap in a pheromone trail will be important. Some moth species use a strategy to continue their search past these points [4] but BMSB strategies are not yet understood.

Conclusion

Pheromone dispersion from a novel brown marmorated stink bug (BMSB) trap was modelled. Compared to the current lure-plus-A4-sticky-panel design, the self-orienting design produces a narrower, more concentrated plume. This is expected to provide a clearer trail for the bugs to follow. Dispersion of the pheromone plume was modelled in three environments: flat and featureless plain, car yard, and vegetation canopies. The canopy strongly disperses the plume. Trap height is important if the plume is to penetrate vegetation. Further studies are needed: higher mesh resolution, higher wind speeds, and more realistic environments. Better understanding of the behaviour of BMSB is needed, particularly the lowest concentration of pheromone they can detect and how they behave when they encounter a local maximum or a gap in a pheromone trail.

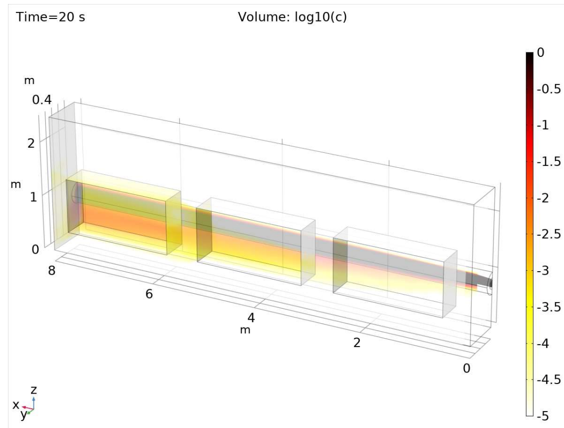

Figure 10. Plume concentration in the simplified car yard.

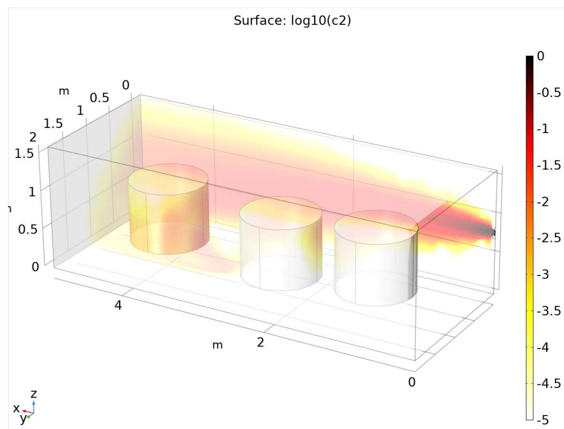

Figure 11. Plume concentration in the simplified vegetation canopies.

Acknowledgements

The authors wish to thank Better Border Biosecurity (B3) (www.b3nz.org) for financial support for this research.

References

[1] Suckling, D.M., Levy, M.C., Roselli, G., Mazzoni, V., Ioriatti, C., Deromedi, M., Cristofaro, M. and Anfora, G., 2019. "Live traps for adult brown marmorated stink bugs." *Insects*, *10*(11), p.376.

[2] COMSOL, 2019. Comsol multiphysics® v. 5.5 www.comsol.com. Stockholm, Sweden. *COMSOL AB*.

[3] Majdoubi, H., Boulard, T., Fatnassi, H., Bouirden, L., 2009, "Airflow and microclimate patterns in a one-hectare Canary type greenhouse: An experimental and CFD assisted study", *Agricultural and Forest Meteorology*, 149(6–7), p. 1050-1062, https://doi.org/10.1016/j.agrformet.2009.01.002.

[4] Cardé RT, Willis MA (2008) Navigational strategies used by insects to find distant, wind-borne sources of odor. J Chem Ecol 34: 854–866